A proof of the direct hole transfer in photocatalysis: The case ofmelamine

(Article begins on next page)

11 July 2024

A PROOF OF THE DIRECT HOLE TRANSFER
IN PHOTOCATALYSIS: THE CASE OF MELAMINE

Valter **Maurino**, Marco **Minella**, Fabrizio **Sordello**, Claudio **Minero***
Chemistry Department and NIS Centre of Excellence, University of Torino, Via P. Giuria 5, Torino, 10125, Italy.

Corresponding author: E-mail: claudio.minero@unito.it; Tel: +39 011 6708449; Fax: +39 011 6707615; Web: http://www.environmentalchemistry.unito.it

ABSTRACT

The photoinduced transformation of 2,4,6-triamino-1,3,5-triazine (melamine) was studied by using different advanced oxidation technologies under a variety of experimental conditions. The systems involving homogeneous hydroxyl radicals, as generated by $H_2O_2/h\nu$, Fenton reagent, and sonocatalysis are ineffective. However, melamine is degraded under photocatalytic conditions or by $SO_4^{\bullet-}$ ($S_2O_8^{2-}/h\nu$). The time evolution of long-living intermediates, such as 2,4-diamino-6-hydroxy-1,3,5-triazine (ammeline) and 2-amino-4,6-dihydroxy-1,3,5-triazine (ammelide), has been followed, being 2,4,6-trihydroxy-1,3,5-triazine (cyanuric acid) the final stable product. During both photocatalytic and $S_2O_8^{2-}/h\nu$ experiments, in the early steps, a fairly stable intermediate evolving to ammelide is observed in a large extent. This intermediate was identified as 2,4-diamino-6-nitro-1,3,5-triazine. This indicates that the primary photocatalytic event is the oxidation of the amino-group to nitro-group through several consecutive fast oxidation steps, and that a hydrolytic step leads to the release of nitrite in solution. To elucidate the nature of the oxidant species hole scavengers such as methanol and bromide ions were added to the irradiated TiO_2. They completely stop the degradation, whereas chloride and fluoride ions decrease the degradation rate.

The study of the photocatalytic degradation rate of melamine at increasing concentrations using two different commercial titanium dioxides, such as P25 and Merck TiO_2, showed an intriguing behavior. A drastic abatement of the melamine transformation rate was observed when coagulation of the P25 slurry occurs due both to the pH change and melamine concentration effect that increase melamine adsorption. In the presence of TiO_2 (Merck) the melamine initial degradation rates are significantly lower than those observed in the presence of P25 but are not depressed at larger concentrations. The experimental evidences (e.g. absence of melamine adsorption onto TiO_2 surface at low concentrations or at acidic pH or due to the catalyst surface texture, and the lack of reactivity toward $^{\bullet}OH$ free and bound) suggest that the effective photocatalytic mechanism is based on an outer sphere direct hole transfer to the melamine. Its formal potential lies in the range 1.9-2.3 V vs NHE. Then, the photodegradation of melamine is an efficient tool to evaluate the direct hole transfer ability of a photocatalyst.

Keywords: photocatalysis, melamine, hydroxyl radicals, TiO_2, Advanced Oxidation Technologies, fluorinated titania.

1 INTRODUCTION

The photocatalytic transformation of several s-triazine derivatives has been extensively investigated.[1,2,3] s-Triazine derivatives have the unique property to lose easily the substituents, but to retain the s-triazine ring till to the formation of 2,4,6-trihydroxy-1,3,5-triazine (cyanuric acid), which is stable to further photocatalytic oxidation.[1] Interestingly, other oxidation processes like UV/H_2O_2 and Fenton reaction lead to stable products that retain the amino group (e.g. from atrazine ammeline is formed) and no cyanuric acid is observed. [4,5] These evidences suggest to study the behaviour of melamine (2,4,6-triamino-1,3,5-triazine) under photocatalytic conditions and in $^\bullet OH$ generating systems.

A preliminary investigation about the $UV/TiO_2/H_2O_2$ melamine degradation was proposed [6] where a not complete mineralization was reported because of the formation of cyanuric acid as last product. An increase of the toxicity during melamine degradation was observed suggesting an undesirable increase of toxicity also during melamine degradation in living tissues. Nothing was reported about the nature of intermediates during the first steps of the photocatalytic process.

In the present paper the photocatalytic transformation of melamine by using different oxidation processes under a variety of conditions is reported. Attention is devoted to the mechanism of oxidation, and in particular to the role of hydroxyl radical vs. direct hole oxidation mechanism. In TiO_2 photocatalysis the role of bound or free $^\bullet OH$ mediated oxidation *versus* direct hole transfer oxidation has been extensively debated [7] and the elucidation of the significance of these pathways has a fundamental importance in the understanding and control of photocatalytic processes. Evidences in support of both mechanisms have been obtained.[8, 9] As far as mechanism is concerned, hydroxyl radical addition or direct electron abstraction can be undistinguishable based on the detected intermediates for most of the substrates.

Some experimental evidences reported on phenol, formate, hydrogen peroxide and glycerol photocatalytic transformations shed some light on these possible pathways.[10, 11] Moreover, they gave insights into the energetics of the surface traps for holes, including also the states associated to adsorbed substrates, and the possibility of water oxidation. It was outlined how the intrinsic and extrinsic surface properties can affect the selectivity of the photocatalytic degradation toward different substrates.[12] Moreover, changes in the extrinsic surface properties, and in particular the adsorption of redox stable ions, influence the relative role of the different paths during the photocatalytic process. Particular attention was devoted to the specific adsorption of fluoride ions (ligand exchange reaction between the surface hydroxy groups and the fluoride ions [11]), which promotes the phototransformation of substrates that react predominantly via $^\bullet OH$ mediated oxidation (e.g. phenol) [7,13], while decreases the degradation rate of substrates (e.g. hydrogen peroxide, catechol) that react predominantly by direct hole transfer mechanism because hinders their specific adsorption.[11,14,15,16] Depending on the substrates, hydroxyl radicals, direct hole transfer (inner or outer sphere) or reductive pathways may operate as initial step and be active all together during the overall degradation process.

A substrate with a high monoelectronic oxidation potential, not reactive toward $^\bullet OH$ radicals and poorly adsorbed onto TiO_2 can help to probe a mechanism that involves a direct hole transfer (likely promoted by shallow surface traps) in photocatalysis. To get information on the hydroxyl radical mechanism, experiments with homogeneous $^\bullet OH$ generating systems were performed. Moreover, attention was devoted to the study of the differences in the photocatalytic activity of TiO_2 P25 and TiO_2 Merck, two different commercial powders with marked differences in their surface features, to highlight the role of the surface properties on the photocatalytic process mechanism. Considering that cyanuric acid is the final product of melamine transformation, this allowed investigating on

the mechanism of $-NH_2$ substitution. Previous studies showed that under photocatalytic conditions the substituents containing nitrogen are redox interconverted ($-NH_2 \rightarrow -NHOH \rightarrow -NO \rightarrow -NO_2$).[17]

2 EXPERIMENTAL

2.1 Materials and Reagents

Melamine (99+%, Aldrich), Cyanuric acid (CYA) (98%, Aldrich) were used without further purification. Ammeline (AN) and Ammelide (AD) were synthesized with the procedure described elsewhere. [1] All other chemicals were commercially available, with at least analytical purity, and used without further purification. TiO_2 P25 by Evonik (formerly Degussa, SSA_{BET} area ca 50 $m^2 g^{-l}$, mixture rutile:anatase 20:80) and TiO_2 by Merck (SSA_{BET} area 10 $m^2 g^{-l}$, anatase 100%) were irradiated in aerated aqueous suspension for at least 12 hours and washed with ultrapure water in order to avoid interference from organic impurities and inorganic ions adsorbed on the photocatalyst. The physical and photochemical properties of the used photocatalyst are reported elsewhere.[18]

Aqueous stock solutions of Melamine (1000 mg dm^{-3}), AN (20 mg dm^{-3}), AD (20 mg dm^{-3}) and CYA (1000 mg dm^{-3}) are fairly stable and last for weeks.

All the aqueous solutions were prepared employing ultrapure water obtained with a MilliQ plus apparatus (TOC = 2 ppb, conductivity 18.2 MΩ cm^{-1}).

2.2 Degradation Experiments

The slurries for photocatalytic experiments were prepared by suspending with sonication the required amount of photocatalyst powder and addition of the needed amount of the aqueous stock solution of substrate. Being 5.5 the natural pH of a TiO_2 suspension (500 mg dm^{-3}) the pH of the slurries before irradiation was adjusted by adding drops of 1 M solutions of NaOH or $HClO_4$ as required.

The irradiation experiments were carried out in Pyrex glass (cut-off at 295 nm) or quartz cylindrical cells (4.0 cm diameter, 2.3 cm height) containing 5 mL of the aqueous suspension of the photocatalyst powder and substrate, using a Philips TLK 40W/05 fluorescent lamp (Phillips, Eindhoven, Nederland) in standard conditions (33 W m^{-2}). This lamp emits a band 60 nm wide, centered at 360 nm (the complete spectrum is reported in [19]). Homogeneous degradation with the H_2O_2 or $S_2O_8^{2-}$/UV systems was carried out in quartz cells, using a Philips 20 W low pressure mercury lamp, emitting at 254 nm. The cell apparatus was described elsewhere.[1] The total photon fluxes in the cells were 7.1×10^{-6} and 7.9×10^{-8} Einstein min^{-1} in the 200-420 nm range with the fluorescent and the mercury lamp, respectively (ferrioxalate actinometry). The cell temperature during irradiation was 30 ± 3 °C. The experiments in the absence of air were prepared purging with He the closed irradiation cells containing either the TiO_2 suspension or water. Then, the required volume of substrate stock solution and, when relevant, the hydrogen peroxide solution were injected in the cell with a microsyringe. During irradiation the slurries were magnetically stirred.

Sonication experiments were conducted with a Branson Sonifier B-15 equipped with standard horn and tip, and a stainless steel sealed 50 mL chamber with cooling jacket. The output setting was adjusted to obtain a 65 Watt output at 20 kHz. The temperature was maintained at 25 °C.

Degradation runs with the Fenton reagent were carried out in the presence of H_2O_2 50 mM and $FeSO_4$ 1 mM at pH 2 (H_2SO_4). The reaction was stopped by adding methanol.

2.3 Analytical Determinations

The HPLC determinations were carried out with a Hitachi Elite Lachrom L2200, equipped with a Diode Array Detector (Hitachi L-2455), on the filtered (Millex HV 0.45 µm, Millipore) irradiated aqueous samples.

Melamine, AN, AD and CYA were quantified with ion pair chromatography with a bonded phase octadecylsilica column (LiChrospher R100-CH 18/2 by Merck, 250 mm length, 10 mm i.d., 5 µm packing); the mobile phase was 0.01 M sodium hexane sulfonate (Aldrich ion-pair reagent 99+%) and 0.014 M H_3PO_4 dissolved in water/CH_3CN 95/5 at 1 mL min^{-1}. Retention times were: melamine 7.8 min, AN 6.8 min, AD 3.1 min and CYA 2.3 min. The detection was carried out at 200 nm for melamine and CYA, at 221 nm for AD and at 229 nm for AN to optimize the analytical sensitivity for each compounds.

The formation of nitrate and nitrite ions was monitored by suppressed ion chromatography, utilizing a Dionex DX500 apparatus equipped with a Dionex AS4-SC separation column and an alkaline buffer eluent containing Na_2CO_3 (1.8 mM) and $NaHCO_3$ (1.7 mM) at the flow rate of 1.5 mL min^{-1}. Ammonium ion quantifications were performed using the Berthellot reagent (Merck) following the procedures suggested by the vendor.

An aqueous solution of 2,4-diamino-6-nitro-1,3,5-triazine (Compound I) was synthetized for the first time irradiating for 40 minutes 1000 mL of a suspension containing melamine (10 mg L^{-1}) and the photocatalyst in the same conditions employed for the melamine photodegradation. After irradiation the suspension was filtered (HV 0.45 µm, Millipore) and freeze-dried. The solid was dissolved in water (40 mL), the residual melamine was precipitated with the stoichiometric amount of cyanuric acid. The solution of I, impure for AN and AD, was purified by chromatography employing a column (500 mm length, 10 mm i.d., Superformance, Merck) packed with octadecylsilica (40-63 µm diameter, irregularly shaped, Merck). The purification runs were carried out on 2 mL aliquots of the solution of I, with ultrapure water as eluent (flow rate 4 ml min^{-1}). The column eluate was monitored with an UV detector ($\lambda = 220$ nm, Hitachi model L4200). The fractions containing I (confirmation was obtained by analytical HPLC) were pooled and freeze dried.

Mass spectra were recorded with a Finnigan-MAT 95Q (Bremen, Germany) hybrid instrument, with BEQ geometry. The ions were collected at the first dynode-electron multiplier detector, located after the magnetic and electrostatic analyzers. The sample was introduced with a direct insertion probe, heated until a constant sample vapor pressure was produced in the ion source. Electron impact (EI) mass spectra were obtained at 70 eV electron energy and 1.0 mA electron current. The mass analyzer was scanned from m/z 29 to m/z 300. Positive chemical ionization (CI) conditions were established by admitting isobutane in the ion source, as the reagent gas, at a pressure of 50 Pa (0.5 mbar). With this pressure, the ratio between m/z 57 and m/z 43 peaks was 10:1. The electron energy was set to 200 eV and the electron current to 0.2 mA. The resolution was set to m/Δm 1000 (5% valley) and the ion source temperature to 220 °C. Electron capture chemical ionization (EC-CI) experiments were carried out in the same conditions except for the polarity of the ion-source and detector voltages, which were reversed to detect negative ions.

3 RESULTS AND DISCUSSION

3.1 Identification of intermediates and final products of melamine photocatalytic degradation

Melamine disappearance followed pseudo-first order kinetics over at least two half-lives in all conditions studied. When persulfate acted either as electron scavenger or photoactivable oxidant, or other reactive chemicals were added to the system their

concentration did not vary significantly during the time interval in which melamine disappeared.

Fig. 1 shows the time profiles of melamine disappearance and product formation under the conditions presently investigated (the photocatalytic experiments were carried out with P25 TiO_2 if not differently specified). As already observed in the s-triazine pesticides degradation through Fenton reagent [4], O_3 [5], and heterogeneous photocatalysis [1], many transformation products are formed, among which ammeline, ammelide and cyanuric acid are the major intermediates and final product, respectively. Cyanuric acid turned out to be stable under the present systems (e.g. no variation is observed after 10 hours of photocatalytic conditions, as well as with Fenton reagent, $S_2O_8^{2-}$ and sonocatalysis).

In the melamine transformation under photocatalytic conditions an additional long-living intermediate (Compound I) is formed in the early stages of degradation at acidic pH, and particularly at pH 5.5 (Fig. 1B). To investigate its nature, the compound was synthesized by using TiO_2 photocatalysis and purified. Its basic hydrolysis (NaOH 1 M) gives ammeline as sole detectable product and NO_2^- as inorganic nitrogen species. This evidence, together with the mass spectra reported in Fig. 2 (neutral loss of 30 from the molecular ion, presence of a peak at m/z 30 characteristic of nitro compounds, a molecular weight of 156) lead to assign the structure of 2,4-diamino-6-nitro-1,3,5-triazine to the Compound I. Moreover, the formation of a nitro group is confirmed by the appearance of an absorption band with the maximum located at 295 nm in the UV spectrum. The synthesis of Compound I allowed its quantification. Compound I is present at significant concentration also in $S_2O_8^{2-}$/hv system at acid and neutral pH (see later). In basic media Compound I was not observed due to its rapid hydrolysis (half-life of the order of few seconds in NaOH 1 M). At acid pH the detected concentration of Compound I is lower than at quasi-neutral pH due to acid hydrolysis.

The quantification of all long-living intermediates accounted for almost 100% of the mass balance. Besides the time evolution of detected intermediates, Fig. 1 reports also the sum of all by-products concentrations. As the mass balance calculated on detected intermediates is almost stoichiometric, possible other products are short-living and rapidly converted. A mass balance defect is present only at pH 5.5 (Fig. 1B) at times before Compound I appearance, suggesting that some short-living intermediates producing Compound I are formed and not detected.

As inorganic nitrogen-containing species are concerned, the evolution of NO_3^- was followed, which is by far the most important species accounting for 90% of the total released nitrogen after 400 minutes in the melamine degradation with TiO_2/hv (see Fig. 1B). Even aniline in oxygenated solution and in the same conditions gave ca 60% of ammonium ions, and NO_3^- is essentially formed through NH_3 photocatalytic conversion. [17] In the case of melamine (and also AD and AN) carbon atoms are in their highest oxidation number (+4). In comparable cases (e.g. CCl_4 [20], $C(NO_2)_4$ [21]) reductive pathways initiate the photocatalytic degradation, but this is not occurring for melamine as in the absence of an electron scavenger no reaction occurs (see Table 1, entry 4) and because from mass balance there is no evidence of melamine-derived reduced species. Conversely, the presence of $S_2O_8^{2-}$ greatly enhances the degradation rate (entries 11 and 12 of Table 1). In this case please note that $S_2O_8^{2-}$ is ca 200 times more concentrated than O_2 and generates the very active $SO_4^{\bullet-}$ species. The $SO_4^{\bullet-}$ radical produced by reduction of $S_2O_8^{2-}$ is an oxidant species that could increase the reaction rate, and this agrees with the entries 3 and 11 of Table 1. In the presence of $S_2O_8^{2-}$ no significant difference is observed if O_2 is present or not. It turns out that electrons in the conduction band, which could back react with holes and with $-NO_2$ or other oxidized transient species (e.g. the primary product of the electron transfer), are scavenged by O_2 and/or $S_2O_8^{2}$. The reaction in the presence of He (Table 1 entry 12) would not be possible if $S_2O_8^{2-}$ did not act as an electron scavenger (compare with Table 1 entry 4). In addition the results indicate that oxygen is not crucial as found in many

other photocatalytic degradations. [22] This does not exclude that when oxygen is present, it can react with intermediate radical species.

Therefore melamine degradation merely proceeds through an oxidation pathway. The process can only initiate through oxidation of nitrogen (here in −3 oxidation number) and further oxidation of the amino group to −NO_2 with subsequent hydrolytic release of NO_2^- that is rapidly oxidized to NO_3^-. Ammonium ions, which are not originated photocatalytically from nitrate, are formed in very low amount through nitrite reduction.[17] Similar mechanism should operate for the formation of traces of NH_4^+ (always less than 2% of the stoichiometric amount) from AN and AD. Among other nitrogen-containing species, hydroxylamine was not detected even in trace amount. On the basis of the above considerations the scheme of reaction reported in Fig. 3 is proposed for the degradation of melamine in the presence of irradiated TiO_2.

The photocatalytic experiment alone is silent on the mechanism of the primary oxidation step, whichever it is due to an electron abstraction by the valence band hole (shallow trapped) or to a surface deep trapped hole forming first a radical cation, or to a hydroxyl radical addition or hydroxyl radical promoted H-abstraction. The detected first long living intermediate I can be formed by all of these processes.

3.2   Evidences for direct hole oxidation

The melamine initial degradation rates in the presence of other different redox systems are summarized in Table 2.

Experiments carried out using $S_2O_8^2$ /UV at different pH are reported in Fig. 4 and the melamine disappearance rate at entries 1-3 of Table 2. The melamine degradation is faster than with irradiated TiO_2 (Fig. 1) due to the different concentration of the primary oxidant species, but the type and time evolution of intermediates are equivalent, also considering the effect of pH. Also in this case the sum of the concentrations of all detected intermediates accounts for almost 100% of the initial melamine. As for photocatalytic transformation, a mass balance defect is present at neutral pH (Fig. 4B), even more pronounced than before. This can be attributed to the faster reaction rate. A careful comparison of data of cyanuric acid evolution of Figure 1 and 4 shows that at acid and basic pH (although not exactly the same) the formation of cyanuric acid is very similar. A difference is present only at neutral pH (pH 5.5 for TiO_2 and 7 for persulfate), for which the photocatalytic rate is almost twice than that in homogeneous solution. Peroxydisulfate in hot water or under UV dissociates into $SO_4^{\bullet-}$ radical, for which the standard redox potential $SO_4^{\bullet-}/SO_4^{2-}$ is quite large (E°= 2.4 V vs NHE). Because $SO_4^{\bullet-}$ radical is quite efficient in promoting the melamine degradation, this implies that the monoelectronic formal potential of melamine oxidation is <2.4 V vs NHE. It is worth pointing out that $S_2O_8^{2-}$, even in absence of light or metal ions which promote the production of $SO_4^{\bullet-}$, degrades melamine (half-life of 30 days). From a mechanistic point of view, $SO_4^{\bullet-}$ radical acts mainly as an electron abstractor.[23] This radical in unable to oxidize water to hydroxyl radical at acidic/neutral pH as it is evident from the standard redox potentials reported in Table 3.

On the basis of the above considerations the scheme of reaction reported in Fig. 3 is confirmed for the degradation of melamine with $S_2O_8^{2-}$/UV, in which the crucial step is melamine oxidation to 2,4-diamino-6-nitro-1,3,5-triazine through a mechanism of electron abstraction for $S_2O_8^{2-}$. Possibly the electron abstraction mechanism is valid also for TiO_2 photocatalysis. The first oxidation step is possibly the formation of a radical cation, which via some intermediates apparent from the mass balance defect, rapidly evolves to Compound I by further oxidation.

Experiments in which $^\bullet OH$ radical is formed (see entries 4-6 in Table 2) demonstrate that oxidation of melamine by $^\bullet OH$ radical attack (both addition and H-abstraction) is not

possible. Electrochemical treatments with high oxygen overvoltage anodes (cell voltage of 4.0 V) proved to be ineffective for melamine oxidation [24], although these conditions produce relatively high concentration of hydroxyl radicals in the proximity of the electrode. Free hydroxyl radical does not react through electron transfer, due to the high reorganization energy associated with transfer of charge.[25]

When generated by H_2O_2 photolysis, the hydroxyl radical concentration is predominantly controlled by the reaction with H_2O_2. Using the value of the kinetic constant reported (k = 2.7×10^7 M^{-1} s^{-1}) [25], the quantum yield of 0.5 and the photonic flux in the cell (7.1×10^{-6} Einstein min^{-1}), concentrations of $^{\bullet}OH$ ranging from 2×10^{-11} M to 5×10^{-11} M are calculated when H_2O_2 initial concentration ranges from 0.01 to 0.1 M. Thus, under these conditions if the second order rate constant of $^{\bullet}OH$ radical with melamine would be at least of the order of 10^4, the rate would be $2-5 \times 10^{-10}$ M s^{-1}; if compared with values of Table 1, melamine would slightly disappear in the time windows of the experiment. Conversely no reaction was observed in the presence of H_2O_2/hv, indicating an insignificant reactivity of $^{\bullet}OH$ radical with melamine (k < 10^4). The Fenton reagent is usually quite effective under the adopted condition to oxidize organic substrates. The Fenton reaction yields both $^{\bullet}OH$ (about 60% at pH 2) and ferryl (about 40%) radicals, where $^{\bullet}OH$ alone is reactive, as recently assessed by a kinetic study.[26] Thus in conditions similar to those of H_2O_2/hv, the previous considerations also apply.

Application of ultrasounds to aqueous solutions induces acoustic cavitation (bubble nucleation, growth, and implosive collapse). Inside the collapsing microbubbles, temperature and pressure increase up to very high values, inducing the pyrolysis of water vapour and of the volatile organic compounds that can be present in the gas phase. Pyrolysis of water vapour yields hydroxyl radicals and hydrogen atoms. Reactions can take place in the gas phase, at the gas-liquid interface, and in the solution bulk after transfer of gaseous radicals into the liquid phase. Although quantification of $^{\bullet}OH$ radical is a difficult task, under similar conditions quite refractory molecules are degraded.[27] With melamine as substrate no reaction is observed.

From the above experiments (entries 4-6 of Table 2) it clearly emerges that only heterogeneous photocatalysis on TiO_2 and systems generating $SO_4^{\bullet -}$ radical can initiate the degradation of melamine, and that in the presently investigated time-domain and for the photocatalytic experiments, hydroxyl radicals, both free in solution, if present, and adsorbed, are not able to react with melamine or at least to generate a transient intermediate evolving toward other more stable species. This confirms that the only possible first step of melamine oxidation is the formation of the radical cation by direct electron abstraction.

Consequently, the mechanism for the primary photocatalytic degradation step is a direct electron abstraction by TiO_2 photo-generated holes. This possibility is supported by Nosaka et al. when they suggest that spin-trapping agents react with surface-trapped holes [9] and not with supposed free $^{\bullet}OH$ radical. Further substantiation of this statement comes out from the results obtained in the photocatalytic experiments in the presence of hole scavengers (entries 7, 8 and 9 in Table 1). Hole scavengers, added at concentration 500-1000 times higher than melamine, transform the photogenerated oxidant species in other radical species unable to set off the melamine degradation. The presence of CH_3OH or bromide completely suppresses the process.

Considering the big difference between the substrate and the hole scavenger concentration and that the reaction with melamine would be a minority path, the photo-formed holes are quickly scavenged by methanol or bromide. The formed radicals are unable to react with melamine. The standard reduction potentials for the couples $E^{\circ}_{Br^{\bullet}/Br-}$ =2.0 V vs NHE and $E^{\circ}_{Br2^{\bullet -}/2Br-}$ =1.7 vs NHE are apparently too low for oxidizing the melamine (see Table 3). In the presence of chlorides, for which the standard reduction

potentials are larger ($E°_{Cl-\bullet/Cl-}$ =2.6 V *vs* NHE, $E°_{Cl2\bullet-/2Cl-}$ =2.3 *vs* NHE)), melamine oxidation is still possible, although the degradation rate is significantly reduced. This observation implies that the standard reduction potential $E°_{MEL+\bullet/MEL}$ is larger than that of $Br_2^{\bullet-}/2Br^-$ couple (1.7 V) and lower than that of $Cl_2^{\bullet-}/2Cl^-$ couple (2.3 V). Having this standard redox potential melamine could be thermodynamically oxidized (see Table 3) by persulfate (and this happens) and by $^\bullet OH$ radicals (and this does not happen for kinetic restrictions as above discussed).

3.3   The hole transfer at the TiO$_2$ surface

The electron transfer across the interface is at the heart of redox photocatalysis as recently reviewed.[28] Electron transfer is an interfacial phenomenon between a surface trapped charge carrier and a chemisorbed or physisorbed species. The complex interplay of the surface texture and the system pH, which affects the main surface species and the melamine charge, prompted us to investigate the effect of pH, melamine concentration, surface modifiers and two different TiO$_2$ specimens to figure out the surface species responsible for the electron transfer.

There are many reports dealing with the thermodynamic of the adsorption on TiO$_2$ surface. Chemical adsorption (surface complex formation) on TiO$_2$ surface occurs when the substrate has oxygen containing groups like carboxylate or alcoholic functions. The review by Thornton et. al [29] reports many of these cases, and in particular the cases of HCOOH and C2-C8 alcohols. As this is not the case for melamine for which only amino-groups are available, melamine is not chemisorbed onto TiO$_2$. Experiments carried out with 2 g L^{-1} TiO$_2$ P25 and 1×10^{-4} M let in the dark for 12 h showed no appreciable decrement of the solution concentration. Then an outer sphere electron transfer can be suggested as primary mechanism for the first step of melamine photocatalytic transformation.

Fig. 5 shows the initial degradation rate of melamine as a function of the initial substrate concentration under different photocatalytic conditions in the presence of TiO$_2$ P25. The photocatalytic melamine transformation was studied in a wide concentration range that covers two orders of magnitude (from 1×10^{-5} to 1×10^{-3} M) at different pHs (3, 5.5 and 11), in the presence or in the absence of fluoride ions and NaClO$_4$ 10^{-3} M.

At pH 3, 11 and at pH 3 in the presence of fluorides (total fluoride concentration 10 mM) the common saturation-type kinetics was observed. The increasing rate vs. substrate concentration is also noticed at low concentration at pH 5.5. The sudden decrease at this pH will be discussed later. The modelling of all the processes occurring at the semiconductor–electrolyte interface is elsewhere reported [30,31] and critically reviewed.[32] The observed Langmuir-Hinshelwood-like dependence of the rate is not due to the substrate adsorption, but derives from the recombination of charge carriers. From the quoted kinetic models the rate should follow a square root dependence on the substrate concentration. In the inset of Fig. 5 a log/log plot is presented. It is apparent that the found slope for data at pH 3 and 5.5 has the predicted dependence for substrates that are not chemisorbed. In the case of chemisorption the rate dependence on concentration is much more complex. An enlightening example is glycerol [10], for which after an initial increase of the rate at low concentration, this decays and later increases again. Then the observed trend of the rate is compatible with a substrate that does not chemically adsorb.

Coming back to the possible involved surface species, depending on the TiO$_2$ specimen, different types of terminal and bridging OH groups could be present on TiO$_2$ [11] that can trap photogenerated holes.

The schematic Ti(OH)(OH) for the (TiO$_2$) unit at the surface resumes many of the possible surface forms that can trap the hole.[28] The unit surface Ti(OH)(OH) can trap holes as (Ti(O$^\bullet$)(OH)) ⇆ (Ti(OH)(O$^\bullet$)), where the first (OH) refers to linear hydroxyl groups

and the right (OH) to bridged hydroxyl groups.[28] In the framework of water oxidation, several other forms have been proposed, like $[Ti_2=O-Ti]_s$ and $[Ti-O-Ti]_s$ that refer to a triply coordinated O atom and a bridging O atom at the surface, respectively.[33] For the trapped hole the form $[Ti-O^\bullet\ HO-Ti]_s$ was also proposed suggesting the possibility that surface oxygen is included in oxidation products. The schematic picture of hole trapping as $(Ti(O^\bullet)(OH)) \leftrightarrows (Ti(OH)(O^\bullet))$ is useful only for a general discussion of the electron transfer process and loses many details as above. The hole trapping as $Ti(O^\bullet)(OH)$ is assumed important only at pH>13 and the most probable hole localization is $Ti(OH)(O^\bullet)$, i.e. on bridged oxygen.

The $Ti(OH)(OH)$ can be protonated/deprotonated at various extent depending on solution pH. Detailed studies on surface oxygen species in a pH range 2.3-11.7 by internal reflection FTIR spectroscopy reported that terminal hydroxyl Ti-OH is present in a pH range from 4.3 to 10.7 (maximum =8), that $Ti-OH_2^+$ exists in a pH range below 5, and $Ti-OH^+-Ti$ exists in a pH range below 4.3. [34] At low pH the surface will be protonated with a positive charge repelling positively charge protonated melamine. The pK_a of melamine is 5.0 [6,35] indicating that at pH below 4 the prevalent form is the protonated one.

The above reported hole trapping scheme outlines the role of solution pH on the electron transfer rate.

The maximum rate observed at pH 5.5 can be explained as the result of the interplay among the valence band edge potential shift, the substrate acid – base properties and the amphoteric properties of the TiO_2 surface (for P25 TiO_2 pzc $\approx$ 6.3).[36] The TiO_2 CB edge exhibits Nernstian dependence with pH, shifting about -60 mV per pH unit in a wide range of pH [37] starting from E_{vb}(pH=0) = 3.0 V vs NHE for anatase.[38] As the surface is positively charged, the electron abstraction from $Ti(OH_2^+)(OH)$ is more difficult, implying that the hole trap $Ti(OH_2^+)(O^\bullet)$ is shallower than $Ti(OH)(O^\bullet)$.[28] From this it follows a greater potential difference with the redox potential of the substrate to be oxidized and a greater reaction rate, if additional effects due to the electrostatic interaction with the surface are not present. Because the electron abstraction is quite disfavored from the protonated melamine, the redox reaction must involve neutral melamine. Considering the pK_a of melamine [6,35], at pH below 4 the prevalent form (more than 99 %) is the protonated one. The decrease in the degradation rate at pH 2.0 with respect to pH 5.5 would follow the melamine speciation and the rate is expected to be dramatically depressed. As this is not the case, it must be hypothesized that the melamine near the surface is in the not protonated form. This is possible only if melamine is not chemisorbed, but resides in the double layer faced to the positive surface where the actual concentration of protons is lower than in solution. In addition, the protonated surface is richer in hydrogen atoms, which increase the possible hydrogen bonding with melamine. These effects partially counterbalance the electrostatic repulsion between the catalyst surface and the protonated melamine, and add to the increase in the driving force discussed above (shallower trap) and guessed by the Marcus-Hush theory.[8]

For basic pH the rate is depressed with respect to acid pH. At basic pH the $Ti(O^-)(O^\bullet)$ is stabilized, as an electron is easily abstracted from a negative surface. This implies a lower oxidizing potential and reduced trapped hole reactivity. No data on the second dissociation of melamine are available [35], and a further dissociation is hardly envisaged leading to a negative charged imide form. The possible additional adverse effects due to the electrostatic repulsion with the negative surface can be present implying a lower rate. For the extreme investigated pH E_{vb}=2.29 V at pH 12 and E_{vb} =2.88 V at pH 2.0. Since at pH 12 melamine transformation was still observed (entries 1,3,4,5 and 6 in Table 1), even if with a rate decrease of an order of magnitude with respect to pH 5.5, it follows that the redox potential for electron abstraction from melamine is $\leq$ 2.3 V, as already suggested above from the effect of chloride addition.

The rate dependence on melamine concentration at pH 5.5 shows a sudden decrease. In the presence of NaClO$_4$ 10^{-3} M at pH 5.5 the same is observed also at very low melamine concentration. The effect is not observed at lower pH. Thus the TiO$_2$ surface should have low adsorption ability toward the perchlorate anion, and the role of NaClO$_4$ would be limited to form a more compact diffusion layer (Guy – Chapman layer) with the decrease of the colloid stability, similarly to other anions. The counterion presence in the double layer strongly changes the water structure at titanium dioxide interface.[39, 40] In Fig. 5 the initial rate evaluation at pH 5.5 was carried out in the absence of a pH buffer so that the pH slightly changes with the increase of the melamine concentration, ranging from 5.5 (melamine initial concentration 1×10^{-5} M) to 6.4 (melamine initial concentration 1×10^{-3} M). The apparent trivial change in the pH values around the TiO$_2$ pzc and the concurrent adsorption of neutral melamine [6] to the surface by hydrogen bond between lateral amino groups and terminal surface hydroxyls cause a shift from the colloid stability regime to a condition where the primary particles coagulate. The possibility of a strong hydrogen bonding with surface hydroxyls is supported by the formation of an insoluble complex with cyanuric acid [41] used for the first time in this work for purification of Compound I, and also suggested above in the discussion of pH effect on the rate. A relevant consequence of the colloid instability is the dramatic decrease of the initial degradation rate of almost an order of magnitude, due mainly to a reduced light harvesting ability of the slurry and possibly to the increased recombination at the particle surface. The effect of colloid size and its light absorption was already reported.[31] In addition, the coagulation of the primary particles generates surface contact points that are active as recombination centres as demonstrated by Gomez and co-workers. [42]

The addition on fluoride ion to the TiO$_2$ slurry at pH 3 (compare the plots in Fig. 5, and entries 2 and 10 in Table 1) significantly reduces the rate for the whole range of melamine concentrations. At C$_0$ = 1×10^{-4} M and pH 3, $r_{pristine}$ / $r_{fluorinated}$ = 4. Under the adopted conditions the saturation of the fluoride adsorption was presumably achieved.[7] The estimated redox potential of the couple $^\bullet$F/F$^-$ is 3.6 V *vs* NHE and makes fluoride stable against oxidation by TiO$_2$ valence band holes, so that its role is a merely surface modification. After the first paper on surface fluorination [7], many paper appeared that have been summarized in a recent review.[28] In general fluorination increases the rate for substrates that react with $^\bullet$OH radicals and depresses the rate for substrates that react by direct electron transfer. As melamine does not react with free $^\bullet$OH, this experiment would support the original [7] and still debated hypothesis, that surface fluorination produces free $^\bullet$OH in solution and impedes hole trapping as Ti(O$^\bullet$)(OH). However an alternative explanation more consistent with all the above discussion is possible.

For substrates that chemisorb, fluoride has a beneficial effect as the back reaction of the adsorbed oxidized substrate with photogenerated electrons is impeded. By means of photopotential decay measurements it was demonstrated that TiO$_2$ surface fluorination retards the reactivity of photogenerated electrons, both for recombination with surface trapped holes and for transfer to oxygen, upward shifts the electronic levels in the potential energy scale, changes the mechanism from direct to indirect for strong adsorbing species, and inhibits the adsorption of intermediates that could serve as recombination centers.[42,43] Chemisorption depresses the photocatalytic rate as demonstrated for glycerol for which different degradation products were observed at large substrate concentration.[10] In the absence of chemical adsorption of melamine at acidic pH (adsorption by hydrogen bonding was supposed above), no displacement of the substrate from the surface can be invoked by fluoride ions. In addition, for the purpose of the present discussion it must be noted that the surface trap Ti(F)(O$^\bullet$) is more shallow than Ti(OH)(O$^\bullet$), and its energy level is more resonant with free holes in the valence band. Then at least none or a moderate positive increase of the reaction rate was expected as for phenol and

benzoic acid.[44] The rate decrease must then be ascribed to the reduced surface accessibility induced by fluoride adsorption which impedes the adsorption by hydrogen bonding and a close contact with surficial bridge oxygen on which holes are shallowly trapped. Then this experiment together with the effect of pH supports the mechanism of direct hole transfer.

Finally, the melamine degradation rate in the presence of P25 and Merck TiO_2 is here compared with the aim to ascertain that what before discussed is not specific of P25. By a comparative FT-IR analysis under various conditions on P25 there are a variety of surface OH, that is at least 3 types of linear hydroxyl groups (in which OH is bound to a surface Ti, let say Ti-OH), and 3 types of bridged hydroxyl groups (Ti-OH-Ti).[11,18] Fig. 6 shows the initial transformation rate at pH 5.5 and 3 as a function of the initial substrate concentration in the presence of TiO_2 Merck. The previously described saturative profile was observed at both pHs for the whole concentration range presently investigated. In the inset of Fig. 6 a log/log plot is presented. It is apparent that the found slope for data at pH 3 and 5.5 has a square root dependence on the melamine concentration as already observed for P25. Comparing the rate of both specimens (Fig. 5 and Fig. 6), it is evident that on TiO_2 Merck the rate is markedly lower by a factor 52 ($C_0 = 1\times10^{-5}$ M) to 23 ($C_0 = 1\times10^{-3}$ M).

Ratios similar to 1 were observed previously with substrates (e.g. phenol) that react predominantly with surface trapped hole (also referred as hydroxyl radical mediated oxidation), while ratios significantly higher than 1 were observed during the photocatalytic transformation of compounds that react predominantly by direct hole oxidation (hydrogen peroxide, formic acid/formate).[11] Considering the different specific surface area between the two investigated catalysts (SSA_{P25} / SSA_{Merck} = 5) it emerges a considerable intrinsic difference in the ability of the two catalysts to promote the degradation, because of the different density of surface traps and surface hydroxyls available for hydrogen bonding. These sites in low coordination conditions are more present on the P25 surface that on Merck TiO_2 [18]. The holes injected at surface defects (borders, corners, steps…) and on (001) plane possibly have both higher redox potential and/or faster transfer kinetics. Then the observed rates agree once again with the direct hole transfer mechanism, as the degradation rate of substrates that react predominantly by direct hole injection are larger on specimens with high density of surface defects.

4 CONCLUSIONS

The comparison of different oxidation processes (photocatalysis, Fenton process, sonocatalysis, H_2O_2/hν, $S_2O_8^{2-}$/hν) showed that only photocatalysis and the generation of $SO_4^{\bullet-}$ are able to transform the melamine. Noticeably, the homogeneous hydroxyl radicals are unable to turn on the degradation process. This makes melamine a peculiar substrate, quite different from the previously tested molecules which react both with free and surface bound $^\bullet$OH, and with valence band holes. From the detailed analysis of the melamine degradation rates under different conditions, it was possible to suggest that the primary degradation step of melamine is an outer sphere direct electron transfer. This feature makes melamine degradation a useful tool to evaluate the direct hole transfer ability of a photocatalyst. The estimated formal reduction potential of melamine is quite large. Then it follows that on TiO_2 surface there is the presence of shallow hole traps with redox potential larger than 2.3 V *vs* NHE. The surface fluorination decreases the physisorption of melamine on the surface and then the reaction rate.

An incomplete mineralization was always observed because the last product of the melamine transformation is the stable and non-toxic cyanuric acid. The formation of 2,4-diamino-6-nitro-1,3,5-triazine (Compound I) as first long living intermediate was observed, indicating that oxidation proceeds on the amino-group till to nitro-group through several

consecutive fast oxidation steps. The hydrolysis of Compound I results in the release of nitrite in solution and initiates processes that gives ammeline, ammelide and cyanuric acid.

In conclusion, the melamine degradation is a useful tool to evaluate the direct hole transfer ability of a photocatalyst. The use of this peculiar substrate can benefit more fundamental studies on the photocatalytic mechanism and also various applications, comprising tests to evaluate the activity of titania photocatalysts.

ACKNOWLEDGEMENTS

TABLES

Table 1 Initial rates of photocatalytic degradation of melamine under different experimental conditions. Melamine initial concentration 1×10^{-4} M, TiO_2 0.5 g dm^{-3}, CH_3OH 0.1 M, Cl^- 0.1 mM, Br^- 0.1 M, total fluoride 1×10^{-2} M, $S_2O_8^{2-}$ 5×10^{-2} M

Entry #	Redox System	Main Active Species	Initial Rate (M s^{-1})
1	pH 2.0, air	$^\bullet OH$, h^+, e^-, O_2^-	8.0×10^{-8} [a]
2	pH 3.0, air	$^\bullet OH$, h^+, e^-, O_2^-	4.5×10^{-8}
3	pH 5.5, air	$^\bullet OH$, h^+, e^-, O_2^-	9.7×10^{-8} [a]
4	pH 5.5, He	$^\bullet OH$, h^+, e^-	no reaction
5	pH 11.0, air	$^\bullet OH$, h^+, e-, O_2^-	4.5×10^{-9}
6	pH 12, air	$^\bullet OH$, h^+, e-, O_2^-	7.2×10^{-9} [a]
7	pH 5.5, CH_3OH, air	$^\bullet CH_2OH$, e^- O_2^-	no reaction
8	pH 2.0, Cl^-, air	$Cl^\bullet$, $Cl_2^{\bullet-}$, e^- O_2^-	2.0×10^{-9}
9	pH 2.0, Br^-, air	$Br^\bullet$, $Br_2^{\bullet-}$, e- O_2^-	no reaction
10	pH 3.0, F^-, air	$^\bullet OH$, h^+, e^-, O_2^-	1.1×10^{-8} [b]
11	pH 5.5, $S_2O_8^{2-}$, air	$^\bullet OH$, h^+, $SO_4^{\bullet-}$, O_2^-	1.2×10^{-6}
12	pH 5.5, $S_2O_8^{2-}$, He	$^\bullet OH$, h^+, $SO_4^{\bullet-}$	1.3×10^{-6}

[a] data from Fig.1
[b] data from Fig. 5

Table 2 Initial melamine degradation rates with different oxidation processes. Melamine initial concentration 1×10^{-4} M; Fenton reagent: H_2O_2 5×10^{-2} M, $FeSO_4$ 1×10^{-3} M at pH 2 (H_2SO_4); H_2O_2 5×10^{-2} M and $S_2O_8^{2-}$ 1×10^{-2} M; all the experiments were carried out under air.

Entry #	Redox System	Main Active Species	Initial Rate (M s^{-1})
1	$S_2O_8^{2-}$/hν (λ=254 nm) pH 1.0	$SO_4^{\bullet-}$	3.5×10^{-6} [a]
2	$S_2O_8^{2-}$/hν (λ=254 nm) pH 7.0	$SO_4^{\bullet-}$	1.0×10^{-5} [a]
3	$S_2O_8^{2-}$/hν (λ=254 nm) pH 13.0	$SO_4^{\bullet-}$	1.1×10^{-6} [a]
4	Fenton Reagent	$^\bullet OH$	no reaction
5	H_2O_2/hν (λ=254 nm), pH 2-6	$^\bullet OH$	no reaction
6	Sonocatalysis (λ=20 kHz, 65 W)	$^\bullet OH$, $H^\bullet$	no reaction

(a) Data from Fig.4

Table 3 Standard reduction potential for selected hole scavengers. [25,45]

Redox couple	Standard reduction potential *vs* NHE
$^{\bullet}F/F^{-}$	3.6 V
$^{\bullet}OH, H^{+}/H_2O$	2.7 V
$Cl^{\bullet}/Cl^{-}$	2.6 V
$SO_4^{\bullet-}/SO_4^{2-}$	2.4 V
$Cl_2^{\bullet-}/2Cl^{-}$	2.3 V
$Br^{\bullet}/Br^{-}$	2.0 V
$^{\bullet}OH/OH^{-}$ (free)	1.9 V
$Br_2^{\bullet-}/2Br^{-}$	1.7 V
$^{\bullet}OH/OH^{-}$ (bound)	1.6 V
$CH_2O, H^{+}/^{\bullet}CH_2OH$	-0.9 V
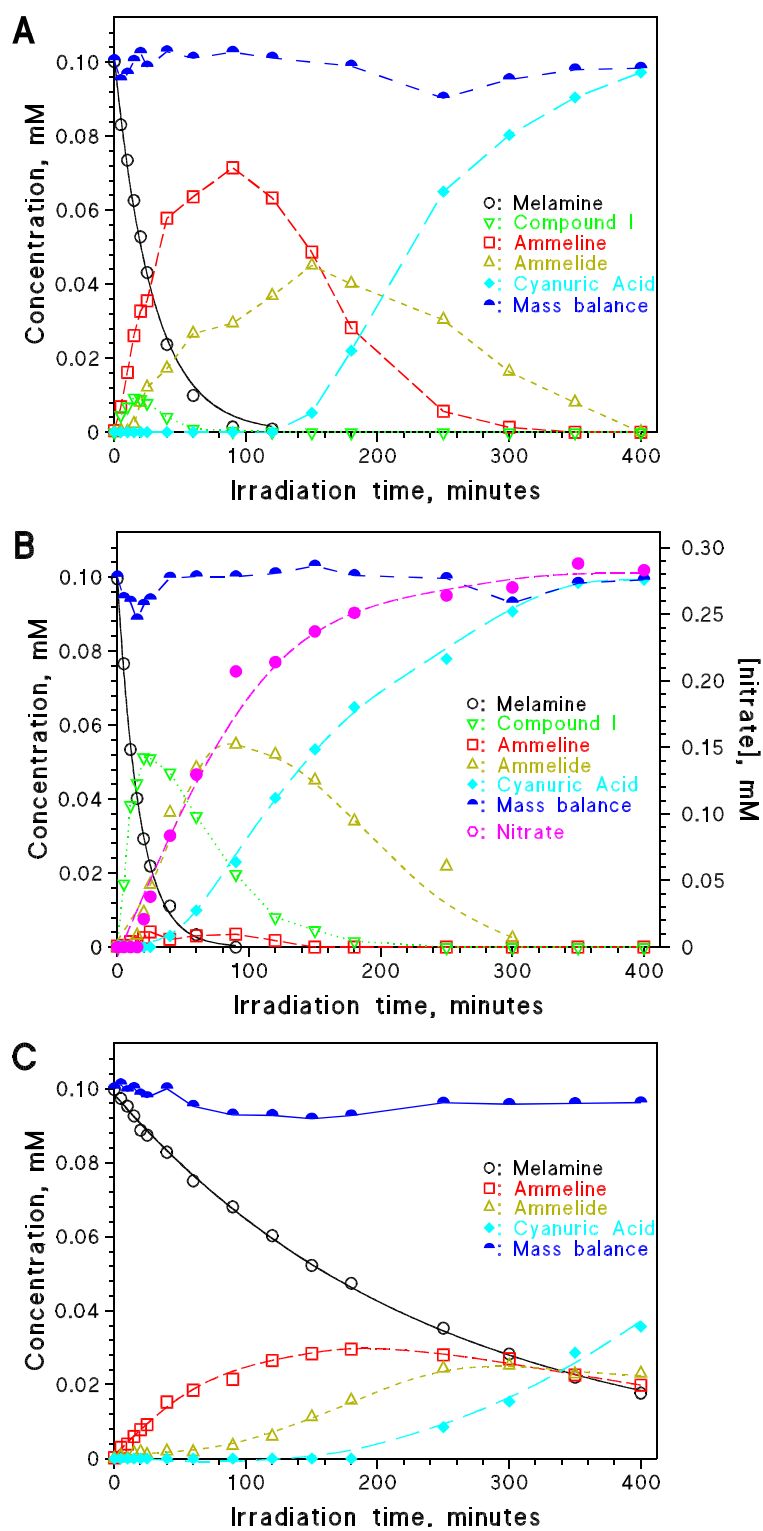
Fig. 1. Photocatalytic transformation of melamine: TiO_2 500 mg dm^{-3}; initial substrate concentration 1.0×10^{-4} M; irradiation at 360 nm. A: pH 2.0 ($HClO_4$); B: pH 5.5 (nitrate concentration refers to the right axis); C: pH 12 (NaOH). The reported mass balance is the sum of concentration of all detected species.
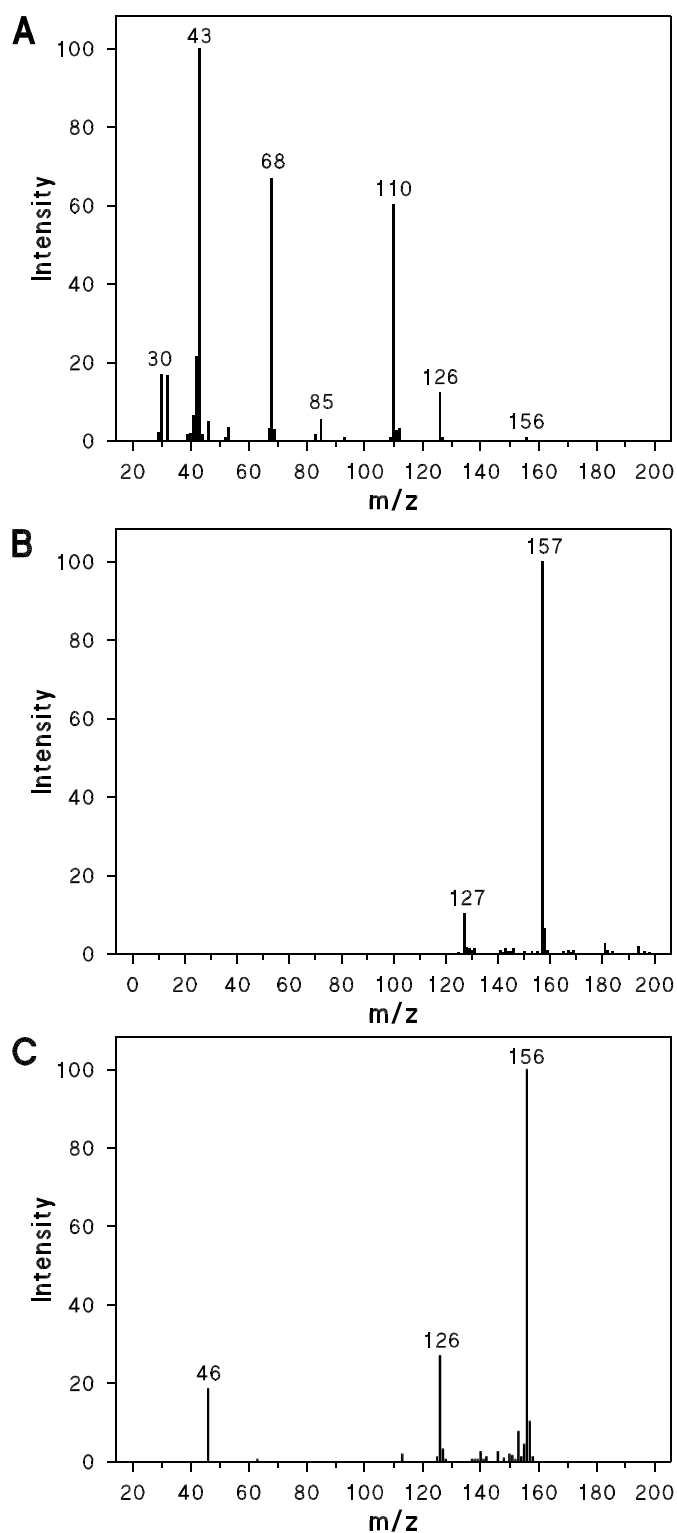
Fig. 2. Mass spectra of compound I. A: Electron impact ionization. B: Positive ion chemical ionization. C: Negative ion chemical ionization. The most characteristic feature of these spectra is the neutral loss of 30 amu fragment from the molecular ion, indicative of the presence of a nitro substituent. The molecular ions suggest a molecular weight of 156 g mol^{-1}, compatible with an s-triazine ring bearing two amino and one nitro group as substituents.
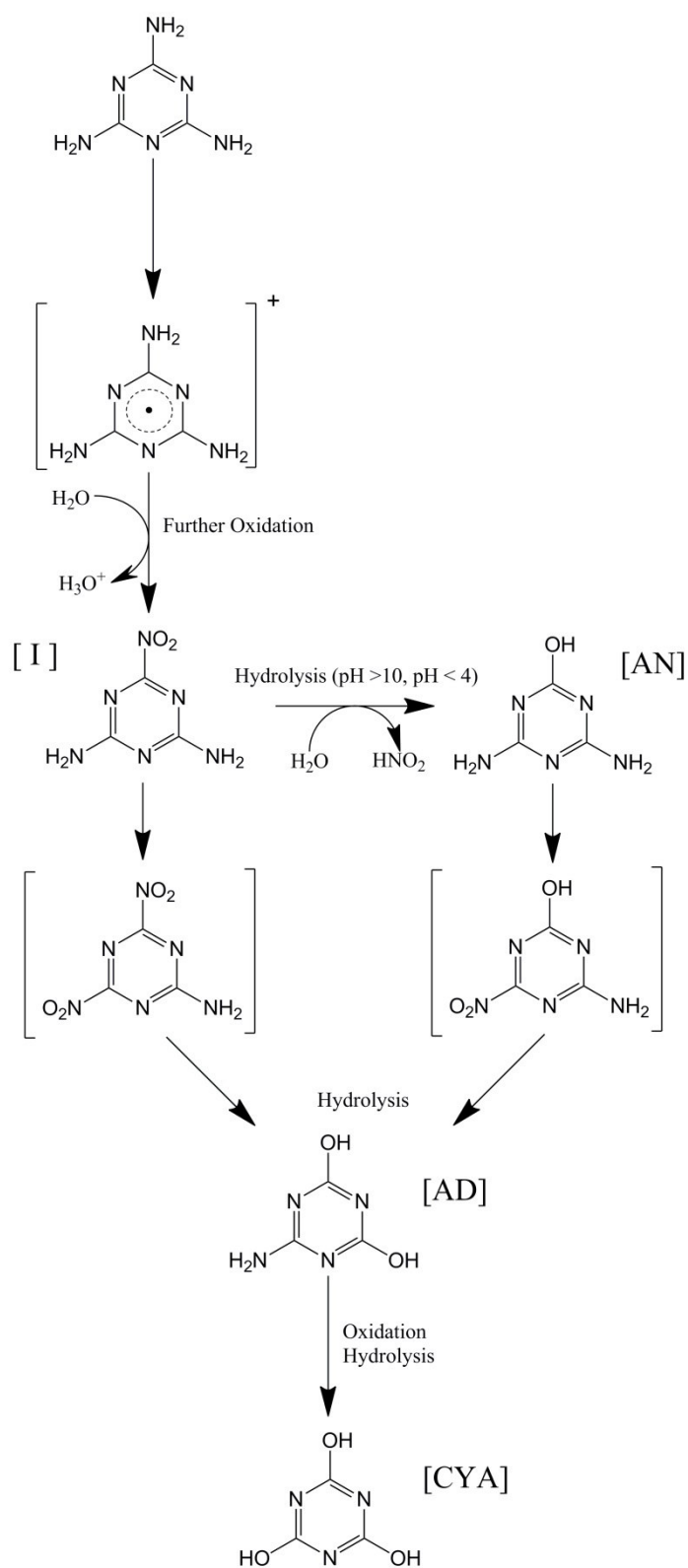
Fig. 3. Proposed pathways for the oxidative transformation of melamine promoted by TiO_2/UV and $S_2O_8^{2-}$/hv. [I] = 2,4-diamino-6-nitro-1,3,5-triazine, [AN] = ammeline, [AD] = ammelide, [CYA] =cyanuric acid. The reported structural formula for AN, AD, and CYA do not correspond to the most stable tautomer (see ref. 35).
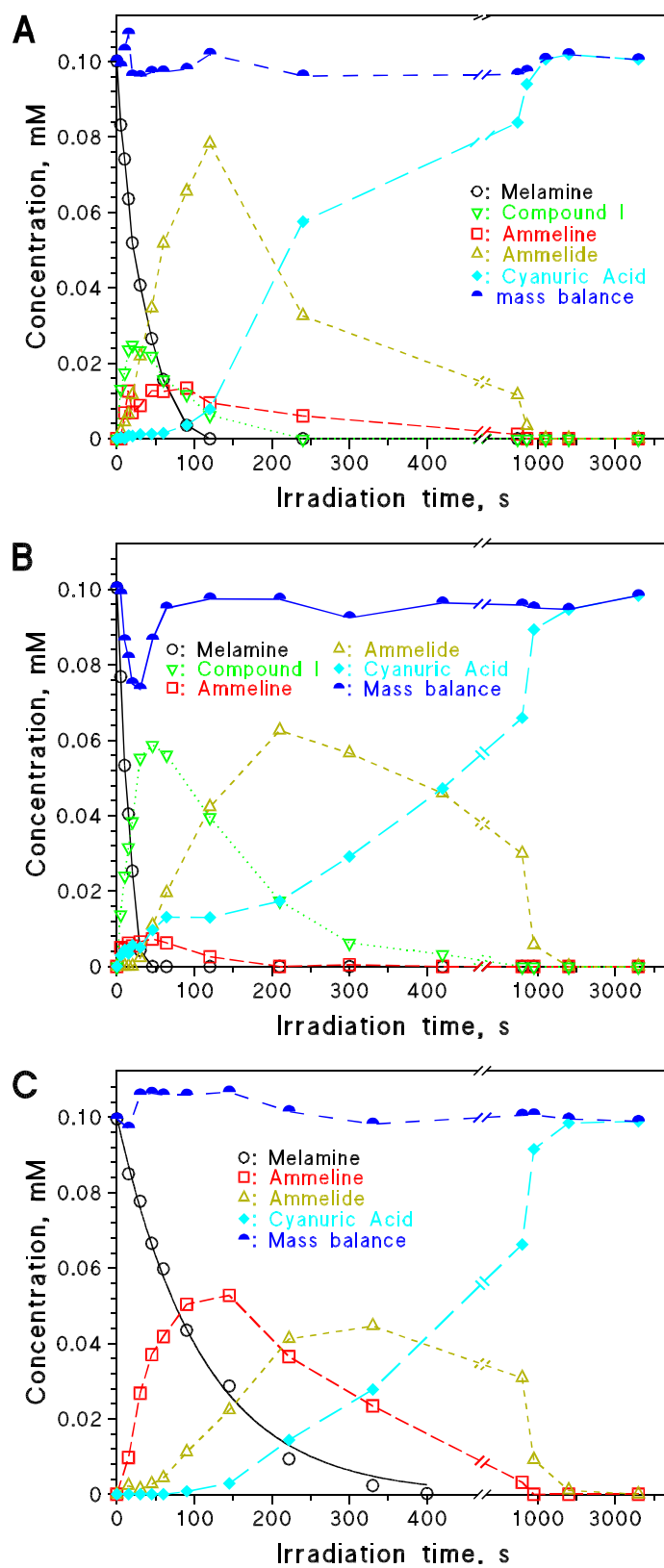
Fig. 4. Melamine transformation in the presence of $S_2O_8^{2-}$ and irradiation at 254 nm. Initial $S_2O_8^{2-}$ concentration: 10 mM; initial substrate concentration: 1.0×10^{-4} M. A: pH 1.0 (H_2SO_4 0.05 M). B: pH 7.0 (phosphate buffer 0.10 M); C: pH 13 (NaOH 0.10 M). The reported mass balance is the sum of concentration of all detected species.
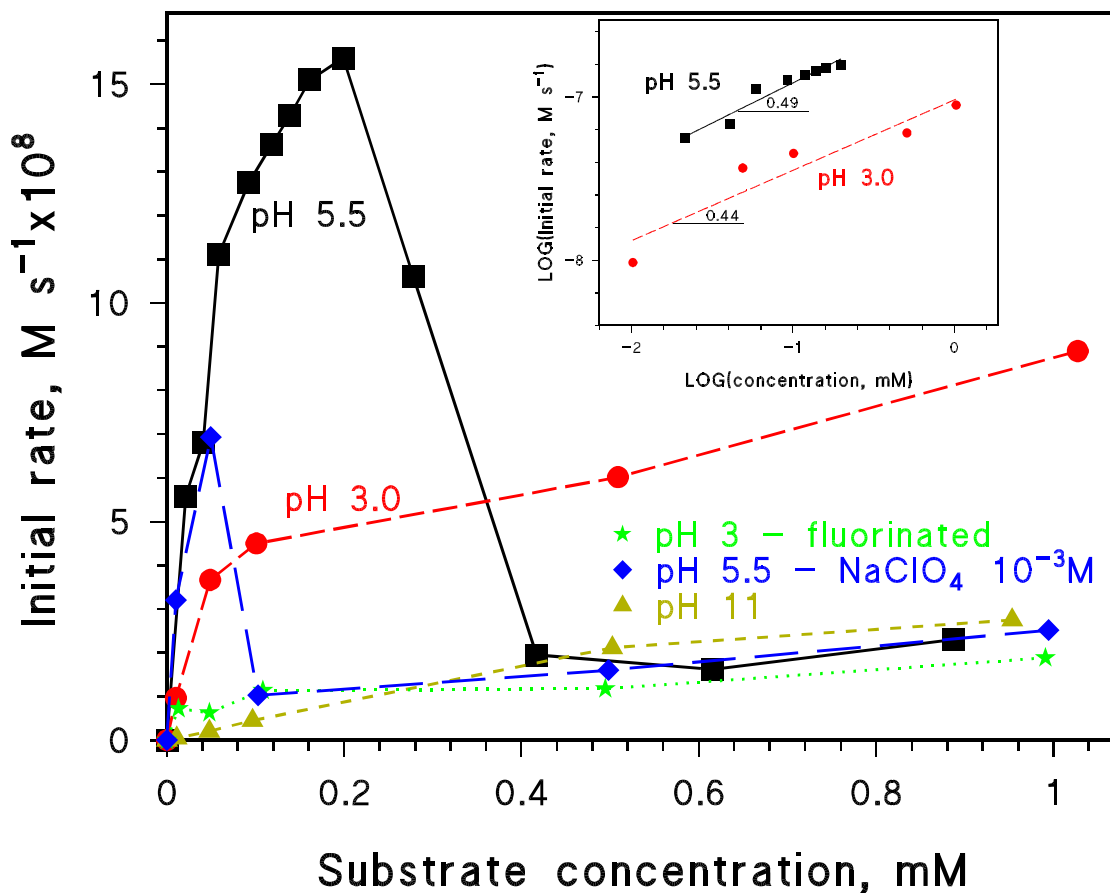
Fig. 5. Initial photocatalytic transformation rate of melamine as a function of the substrate concentration at pH 5.5, pH 3, pH 11, pH 3 in the presence of 10 mM of total fluoride and pH 5.5 in the presence of $NaClO_4$ 10^{-3} M (air, TiO_2 P25 0.5 g dm^{-3}). Inset: logarithmic plot of rates at pH 3 and 5.5 (substrate concentration <0.2 mM).
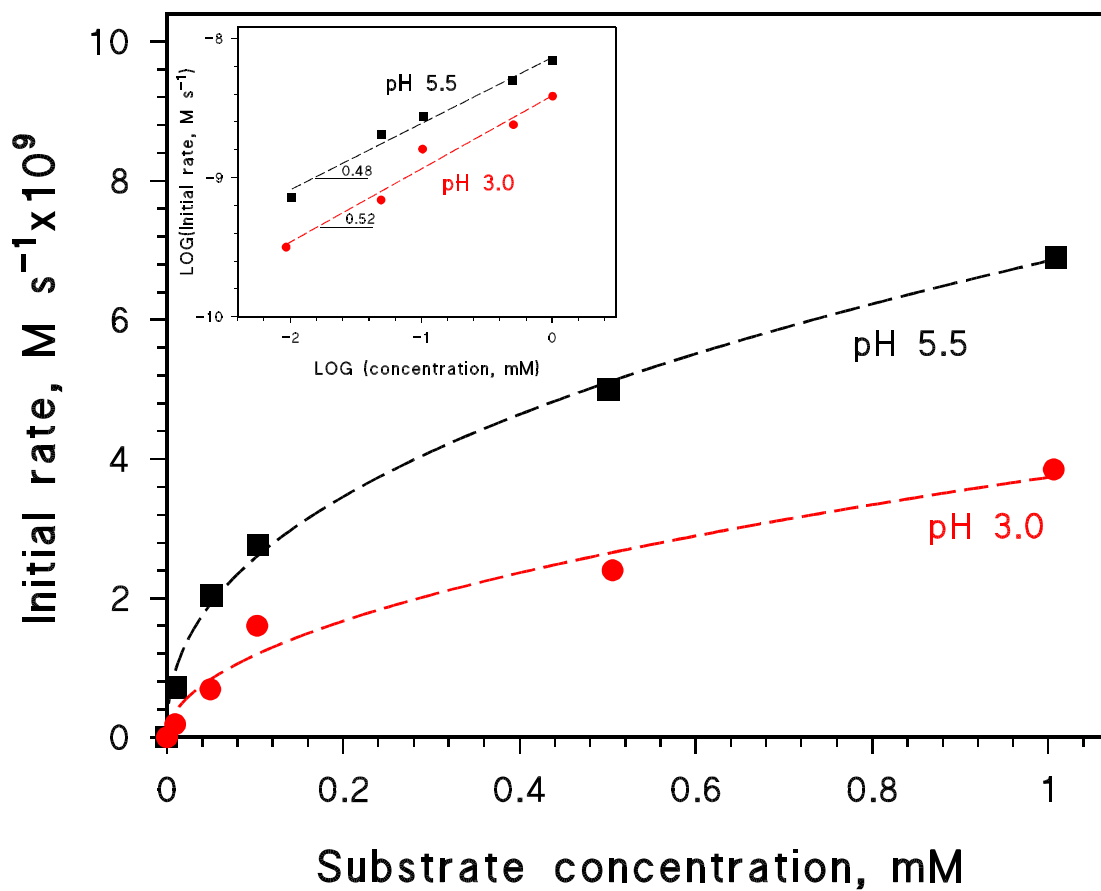
Fig. 6. Initial photocatalytic transformation rate of melamine as a function of the substrate concentration at pH 5.5 and pH 3 (air, TiO_2 Merck 0.5 g dm^{-3}). Inset: logarithmic plot of rates at pH 3 and 5.5.

REFERENCES

[1] E. Pelizzetti, V. Maurino, C. Minero, V. Carlin, E. Pramauro, O. Zerbinati, M.L. Tosato, Environ. Sci. Technol. 24 (1990) 1559–1565.

[2] C. Minero, V. Maurino, E. Pelizzetti, Res. Chem. Interm. 23 (1997) 291–310.

[3] G. Goutailler, J-C. Valette, C. Guillard, O. Païssé, R. Faure, J. Photochem. Photobiol. A-Chem. 141 (2001) 79–84

[4] S.M. Arnold, W.J. Hickey, R.F. Harris, Environ. Sci. Technol. 29 (1995) 2083–2089.

[5] G. Zong, W. R. Lusby, M. T. Muldoon, R. Waters, C.J. Hapeman-Somich, J.Agric. Food Chem. 40 (1992) 2294–2298.

[6] A. Bozzi, M. Dhananjeyan, I. Guasaquillo, S. Parra, C. Pulgarin, C. Weins, J. Kiwi, J. Photochem. Photobiol. A-Chem. 162 (2004) 179–185.

[7] C. Minero, G. Mariella, V. Maurino, E. Pelizzetti, Langmuir 16 (2000) 2632–2641.

[8] M.A. Henderson, Surf. Sci. Rep. 66 (2011) 185–297

[9] Y. Nosaka, S. Komori, K. Yawata, T. Hirakawa, Y.A. Nosaka, Phys. Chem. Chem. Phys. 5 (2003) 4731–4739.

[10] C. Minero, A. Bedini, V. Maurino, Appl. Catal. B-Environ. 128 (2012) 135-143.

[11] M. Minella, M.G. Faga, V. Maurino, C. Minero, E. Pelizzetti, S. Coluccia, G. Martra, Langmuir 26 (2010) 2521–2527.

[12] J. Ryu, W. Choi, Environ. Sci. Technol. 42 (2008) 294–300.

[13] C. Minero, G. Mariella, V. Maurino, D. Vione, E. Pelizzetti, Langmuir 16 (2000) 8964–8972.

[14] V. Maurino, C. Minero, G. Mariella, E. Pelizzetti, Chem. Commun. (2005) 2627–2629.

[15] H. Park, W. Choi, J. Phys. Chem. B 108 (2004) 4086–4093.

[16] M. Mrowetz, E. Selli, New J. Chem. 30 (2006) 108–114.

[17] P. Piccinini, C. Minero, E. Pelizzetti, M. Vincenti, J. Chem. Soc. Faraday Trans. 93 (1997) 1993–2000.

[18] G. Martra, Appl. Catal. A-Gen. 200 (2000) 275–285.

[19] S. Chiron, S. Barbati, S. Khanra, B.K. Dutta, M. Minella, C. Minero, V. Maurino, E. Pelizzetti, D. Vione, Photochem. Photobiol. Sci. 8 (2009) 91–100.

[20] P. Calza, C. Minero, E. Pelizzetti, Environ. Sci. Technol. 31 (1997) 2198–2203.

[21] C. Minero, P. Piccinini, P. Calza, E. Pelizzetti, New. J. Chem. 20 (1996) 1159–1164.

[22] E. Pelizzetti; C. Minero, Colloids Surf., A 151 (1999) 329–338.

[23] P. Neta, R.E. Hule, A.B. Ross, J. Phys. Chem. Ref. Data 17 (1988) 1027–1284.

[24] S. Stucki, R. Kötz, B. Carcer, W. Suter, J. Appl. Electrochem. 21 (1991) 99–104.

[25] G.V. Buxton, C.L. Greenstock, W.P. Helman, A.B. Ross, J. Phys. Chem. Ref. Data 17 (1988) 513–886.

[26] C. Minero, M. Lucchiari, V. Maurino, D. Vione, RSC Adv. 3 (2013) 26443–26450.

[27] N. Serpone, R. Terzian, P. Colarusso, C. Minero, E.Pelizzetti, H. Hidaka, Res. Chem. Interm. 18 (1992) 183–202.

[28] C. Minero, in: D.W Bahnemann, P.K.J. Robertson (Eds.), Environmental Photochemistry Part III, The Handbook of Environmental Chemistry 35 (2015), Springer-Verlag, Berlin Heidelberg, 2013, pp. 23–44.

[29] C.L. Pang, R. Lindsay, G. Thornton, Chem. Soc. Rev. 37 (2008) 2328–2353.

[30] C. Minero, Catal. Today 54 (1999) 205–216.

[31] C. Minero, D. Vione, Appl. Catal. B-Environ. 67 (2006) 257–269.

[32] C. Minero, V. Maurino, D. Vione, in: P. Pichat (Ed.), Photocatalysis and water purification. From fundamentals to Recent Applications, Wiley VCH Verlag GmbH, Weinheim, 2013, pp. 53–72.

[33] A. Imanishi, T. Okamura, N. Ohashi, R. Nakamura, Y. Nakato, J. Am. Chem. Soc. 129 (2007) 11569–11578.

[34] P.A. Connor, K.D. Dobson, A.J. McQuillan, Langmuir 15 (1999) 2402–2408.

[35] Y.H. Jang, S. Hwang, S.B. Chang, J. Ku, D.S. Chung, J. Phys. Chem. A 113 (2009) 13036–13040.

[36] J. Augustynski, Struct. Bond. 69 (1988) 1–61.

[37] A. Fujishima, X. Zhang, D. A. Tryk, Surf. Sci. Rep. 63 (2008) 515–582

[38] M.R. Hoffmann, S.T. Martin, W. Choi, D.W. Bahnemann, Chem. Rev. 95 (1995) 69–96.

[39] S. Kataoka, M.C. Gurau, F. Albertorio, M.A. Holden, S-Mi Lim, R.D. Yang, P.S. Cremer, Langmuir 20 (2004) 1662–1666.

[40] B.P. Nelson, R. Candal, R.M. Corn, M.A. Anderson, Langmuir 16 (2000) 6094–6101.

[41] A. Ranganathan, V.R. Pedireddi, C.N.R. Rao, J. Am. Chem. Soc. 121 (1999) 1752-1753.

[42] D. Monllor-Satoca, R. Gómez, J. Phys. Chem. C 112 (2008) 139–147.

[43] D. Monllor-Satoca, T. Lana-Villarreal, R. Gómez, Langmuir 27 (2011) 15312–15321.

[44] D. Vione, C. Minero, V. Maurino, M.E. Carlotti, T. Picatonotto, E. Pelizzetti, Appl. Catal. B-Environ. 58 (2005) 81–90.

[45] P. Wardman, J. Phys. Chem. Ref. Data 18 (1989) 1637–1755.